Check for updates

Highly efficient CuNi–ZrO$_2$ nanocomposites for selective hydrogenation of levulinic acid to γ-valerolactone†

Yufang Ding, [iD] ‡ Junli Sun,‡ Rongqi Hu, Daiping He, [iD] * Xulin Qiu, Chengying Luo and Ping Jiang [iD]

CuNi–ZrO$_2$ nanocomposites were prepared by a simple coprecipitation technique of copper, nickel and zirconium ions with potassium carbonate. The structures of the nanocomposites were characterized by N$_2$ physical adsorption, XRD, H$_2$-TPR and STEM-EDS. The Cu$_{0.05}$Ni$_{0.45}$–ZrO$_2$ nanocomposite showed outstanding catalytic performance in hydrogenation of levulinic acid (LA) to γ-valerolactone (GVL), especially NaOH solution (0.5 mol L^{-1}) as a solvent. 100% LA conversion and > 99.9% GVL selectivity are achieved over Cu$_{0.05}$Ni$_{0.45}$–ZrO$_2$ catalyst at 200 °C, 3 MPa for 1.5 h. Characterization results suggest that the excellent reactivity of the Cu$_{0.05}$Ni$_{0.45}$–ZrO$_2$ may be due to a better reducibility of nickel oxide in the CuONiO–ZrO$_2$, dispersion of Ni in the Cu$_{0.05}$Ni$_{0.45}$–ZrO$_2$ compared to nickel oxide in the NiO–ZrO$_2$ and Ni in the Ni$_{0.5}$–ZrO$_2$ and promotion of OH$^-$. The results demonstrate that the Cu$_{0.05}$Ni$_{0.45}$–ZrO$_2$ nanocomposite has potential to realize high efficiency and low-cost synthesis of liquid fuels from biomass.

Introduction

Our over-reliance on fossil resources for various chemicals and fuels production has caused global fuel supply deficiency and environmental issues.[1] Transformation of abundant and reproducible biomass to chemicals and fuels can be a promising solution to both issues. Lignocellulose is the most abundant biomass resource on Earth, and is mainly composed of cellulose and lignin. The former can be decomposed into high concentration guaiacol and polyaromatic hydrocarbons by rapid pyrolysis and hydrothermal liquefaction.[1] The latter can be converted into LA, 5-hydroxymethylfurfural and furfural.[2] These molecules can further be converted into useful chemicals and fuels.[3,4] Catalytic hydrogenation of LA to GVL has attracted much attention in recent years because of GVL's unique properties of low toxicity, high boiling point, excellent stability and high energy density, and widespread application as a fuel and food additives, green solvent for synthesis of pharmaceuticals, a versatile building block for production of polymers, olefins and other chemicals with high added value.[5–8]

The hydrogenation of LA to GVL has been reported over both homogeneous and heterogeneous catalysts. The homogeneous catalysts are superior to the heterogeneous catalysts in catalytic reactivity and selectivity toward GVL, but the use of noble metal (Ru, Pd, Rh, *etc.*) complexes limits their applications, and catalyst recovery after reaction is still a major issue. Considering the advantages of the heterogeneous catalysts in recovery and recyclability, different heterogeneous catalysts have been developed to catalyze the hydrogenation of LA toward GVL. Noble metals (Ru,[9] Pt,[10] Pd,[11] Ir,[12] *etc.*) on various supports have been reported to effectively catalyze the reaction. Particularly, supported Ru-based catalysts have been widely investigated for the hydrogenation of LA toward GVL because they exhibited excellent hydrogenation activity and selectivity toward GVL.[13–16] However, the Ru-based catalysts showed deactivation during the LA hydrogenation.[17,18] Base metal catalysts are usually preferred due to their availability and low price, which are more suitable for large-scale use. Various base metal (Cu,[19] Ni,[20] Co[21]) catalysts have been investigated for the LA hydrogenation toward GVL. Rode *et al.* found that the LA could be transformed to GVL with a 100% selectivity on Cu–ZrO$_2$ catalyst under harsh reaction conditions, *i.e.*, high temperatures (200–265 °C), high pressures (3.0–7.0 MPa H$_2$) and long reaction times (5–10 h).[22] Mohan *et al.* reported that the Ni–SiO$_2$ catalyst showed a high GVL productivity,[23] whereas the selectivity toward GVL was 87%.

Herein, we reported the hydrogenation of LA toward GVL on Cu$_{0.05}$Ni$_{0.45}$–ZrO$_2$ nanocomposite in a tank reactor. The catalyst showed rather better performance for the hydrogenation of LA to GVL than Ni–ZrO$_2$, especially Cu–ZrO$_2$ and Ni–SiO$_2$ catalysts.

Chongqing Key Lab of Green Catalysis Materials and Technology, College of Chemistry, Chongqing Normal University, Chongqing 401331, China. E-mail: hedaiping@126.com

Experimental section

Catalyst preparation

Levulinic acid and $Zr(NO_3)_4 \cdot 3H_2O$ (99%) were procured from Chengdu Aikeda Chemical Reagent Co. Ltd $Cu(NO_3)_2 \cdot 3H_2O$ (99%), $Ni(NO_3)_2 \cdot 6H_2O$ (99%) and K_2CO_3 (99%) were obtained from Chengdu Cologne Chemicals Co. Ltd.

The Ni_xCu_y–ZrO_2 nanocomposites with different molar fractions of Cu and Ni ($x + y = 0.5$) were prepared by a coprecipitation technique. Typically, $Cu(NO_3)_2 \cdot 3H_2O$, $Ni(NO_3)_2 \cdot 6H_2O$ and $Zr(NO_3)_4 \cdot 3H_2O$ were dissolved in redistilled water according to nanocomposites components and precipitated using 0.2 mol L^{-1} K_2CO_3 solution under stirring at room temperature. The precipitate was separated by filtration and washed with redistilled water to remove soluble ions after aging the precipitate for 5 h. The precipitate thus obtained was dried for 10 h at 110 °C and calcined for 4 h at 400 °C in an air flow. Then the calcined catalyst was reduced for 2 h at 400 °C in a H_2 flow. The $Cu_{0.05}$–ZrO_2 and $Ni_{0.05}$–ZrO_2 catalysts were prepared in the same manner as that of Ni_xCu_y–ZrO_2. The molar fractions of Cu and Ni in the $Cu_{0.5}$–ZrO_2, $Ni_{0.5}$–ZrO_2 and $Cu_{0.05}Ni_{0.45}$–ZrO_2 were 0.488, 0.493, 0.049 and 0.446 according to ICP-AES determination, respectively.

Catalyst characterization

XRD patterns of catalysts were recorded on a Rigaku D/Max Ultima IVX-ray diffractometer with a 40 kV accelerating voltage and 30 mA current using CuK_α radiation. Their pore structures and specific surface areas were determined *via* N_2 adsorption–desorption on an ASAP 2010 Micromeritics apparatus. Temperature-programmed reduction (TPR) was performed on a Finesorb-3010 chemisorption instrument. 100 mg catalyst was gradually heated to 200 °C and held for 2 h, then cooled to 50 °C in an argon flow of 50 mL min^{-1}. Then the catalyst was heated to 700 °C at 10 K min^{-1} in a H_2/Ar (10% v/v) flow of 40 mL min^{-1}. The effluent gas H_2 is analyzed with a thermal conductivity detector. STEM and EDS measurements were performed on a JEOL JEM 2100 transmission electron microscope at a 200 kV accelerating voltage. XPS spectra were recorded by an X-ray photoelectron spectrometer (ESCALAB 250Xi, AlK_α, C 1s 284.6 eV).

Catalytic tests

Hydrogenation of LA was performed in a telfon-lined stainless steel autoclave. In each run, 10 mL of LA aqueous solution (5 wt%) and 15 mg catalyst was used. The autoclave was purged one time with nitrogen and four times with hydrogen, then it was pressurized to the desired hydrogen pressure. The reaction mixture was stirred at 1000 rpm. The products were determined by GC9890 gas chromatography with a capillary column (SE-30) and flame ionization detector using 1-butanol as an internal standard.

Results and discussion

Catalyst characterization

The textural properties of the $Cu_{0.5}$–ZrO_2, $Ni_{0.5}$–ZrO_2 and $Cu_{0.05}Ni_{0.45}$–ZrO_2 catalysts were determined by N_2 physical adsorption. They showed similar type IV isotherm (Fig. S1†). As displayed in Table S1,† the BET specific surface area, pore volume and mean pore size of the $Cu_{0.05}Ni_{0.45}$–ZrO_2 catalyst were 101 m^2 g^{-1}, 0.18 cm^3 g^{-1} and 3.7 nm, respectively. They were larger than those of the $Cu_{0.5}$–ZrO_2 (85 m^2 g^{-1}, 0.13 cm^3 g^{-1} and 3.6 nm) and the $Ni_{0.5}$–ZrO_2 (94 m^2 g^{-1}, 0.16 cm^3 g^{-1} and 3.5 nm).

The XRD patterns of the $Cu_{0.5}$–ZrO_2, $Ni_{0.5}$–ZrO_2 and $Cu_{0.05}Ni_{0.45}$–ZrO_2 catalysts are shown in Fig. 1. For the $Cu_{0.5}$–ZrO_2 catalyst, four main diffraction peaks were observed. $2\theta = 30.3°$ correspond to tetragonal ZrO_2 phase (JCPDS17-0923),[24] while $2\theta = 43.4°$, 50.4° and 74.2° correspond to the Cu(111), Cu(200) and Cu(220) planes of Cu (JCPDS004-0836).[25] For the $Ni_{0.5}$–ZrO_2 catalyst, three main diffraction peaks were observed at $2\theta = 30.3°$, 50.6°, 60.1° which is attributed to tetragonal ZrO_2 phase, while $2\theta = 44.3°$ and 76.4° correspond to the Ni(111) and Ni(220) planes of Ni (JCPADS#04-0850).[26] The $Cu_{0.05}Ni_{0.45}$–ZrO_2 catalyst showed two main diffraction peaks of tetragonal ZrO_2 phase and metallic Ni at 30.3° and 44.3°. The characteristic peaks of Cu do not appear in the $Cu_{0.05}Ni_{0.45}$–ZrO_2 catalyst. It can be suggested that the Cu are highly dispersed in the nanocomposite. Further analysis of Ni(111) reflection with Sherrer's equation, it was found that Ni crystallite sizes in the $Cu_{0.05}Ni_{0.45}$–ZrO_2 and $Ni_{0.5}$–ZrO_2 catalysts are 3.8 nm and 5.7 nm, respectively. The Ni crystallite size in the $Cu_{0.05}Ni_{0.45}$–ZrO_2 is smaller than that of the $Ni_{0.5}$–ZrO_2, which suggests that the replacement of Cu makes Ni more dispersed in the nanocomposite.

Fig. 2 shows the H_2-TPR profiles of CuO–ZrO_2, NiO–ZrO_2 and CuONiO–ZrO_2. For the CuO–ZrO_2 (Fig. 2a), there was a reduction peak at 200 °C, which is ascribed to the reduction of CuO.[27] The NiO–ZrO_2 and CuONiO–ZrO_2 show reduction peaks at 328–505 °C, which correspond to the reduction of NiO.[28] The reduction peak at 505 °C is probably ascribed to the NiO with relatively strong interaction with ZrO_2. For the CuONiO–ZrO_2, the reduction temperatures of low temperature peaks were obviously lower than those of NiO–ZrO_2, suggesting that the NiO in the CuONiO–ZrO_2 was more dispersed. The reduction peak at 196 °C in the CuONiO–ZrO_2 is ascribed to the reduction of CuO. The reduction temperature is lower than that of CuO in the CuO–ZrO_2. The relatively low reduction temperature is
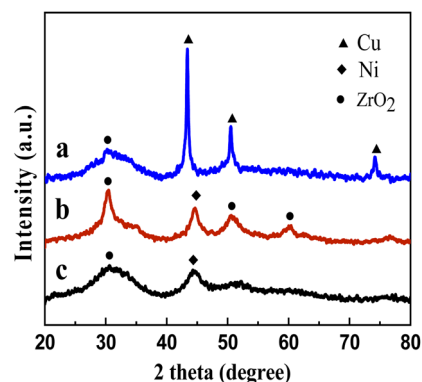

Fig. 1 XRD patterns of the $Cu_{0.5}$–ZrO_2 (a), $Ni_{0.5}$–ZrO_2 (b) and $Cu_{0.05}Ni_{0.45}$–ZrO_2 (c) catalysts.
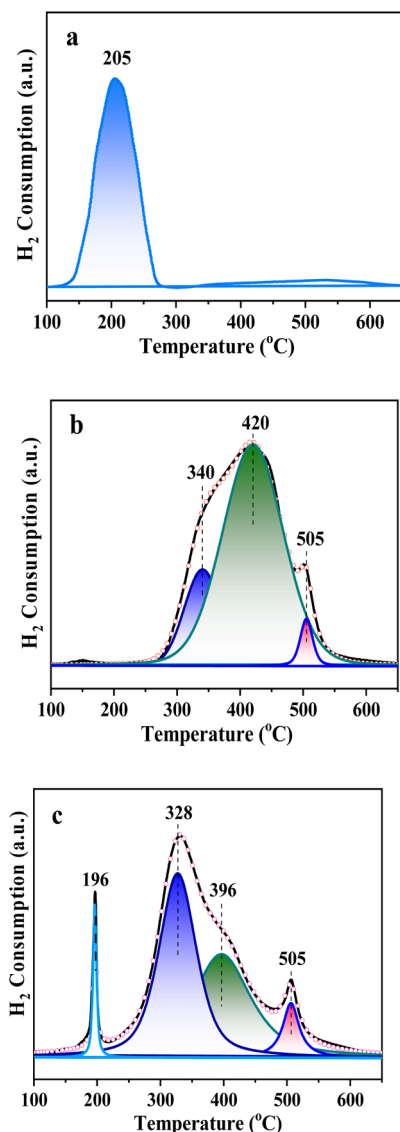
Fig. 2 TPR profiles of the CuO–ZrO$_2$ (a), NiO–ZrO$_2$ (b) and CuONiO–ZrO$_2$ (c) samples.

Fig. 3 TEM images and elemental mapping of the Cu$_{0.05}$–ZrO$_2$ (a–e), Ni$_{0.45}$–ZrO$_2$ (f–j) and Cu$_{0.05}$Ni$_{0.45}$–ZrO$_2$ (k–p) catalysts.

probably due to high dispersion of CuO in the nanocomposite. These are consistent with the results of XRD characterization.

To further identify the microstructures of Cu, Ni and ZrO$_2$, STEM-EDS analysis of the Cu$_{0.5}$–ZrO$_2$, Ni$_{0.5}$–ZrO$_2$ and Cu$_{0.05}$Ni$_{0.45}$–ZrO$_2$ were carried out. The elemental mapping images of the Cu$_{0.5}$–ZrO$_2$, Ni$_{0.5}$–ZrO$_2$ and Cu$_{0.05}$Ni$_{0.45}$–ZrO$_2$ show that Cu, Ni are highly dispersed in ZrO$_2$ (Fig. 3b, g and l). For the Cu$_{0.05}$Ni$_{0.45}$–ZrO$_2$ nanocomposite, the Ni was evenly separated by Cu and ZrO$_2$ (Fig. 3l), suggesting better dispersion of Ni in the Cu$_{0.05}$Ni$_{0.45}$–ZrO$_2$ nanocomposite than that in the Ni$_{0.5}$–ZrO$_2$. This is consistent with the results of XRD and H$_2$-TPR characterizations.

XPS analysis was carried out on the Cu$_{0.5}$–ZrO$_2$, Ni$_{0.5}$–ZrO$_2$ and Cu$_{0.05}$Ni$_{0.45}$–ZrO$_2$ catalysts and the results were shown in Fig. S2 and S3.† The Cu 2p spectra of the Cu$_{0.5}$–ZrO$_2$ and Cu$_{0.05}$Ni$_{0.45}$–ZrO$_2$ can be deconvoluted into two peaks, respecti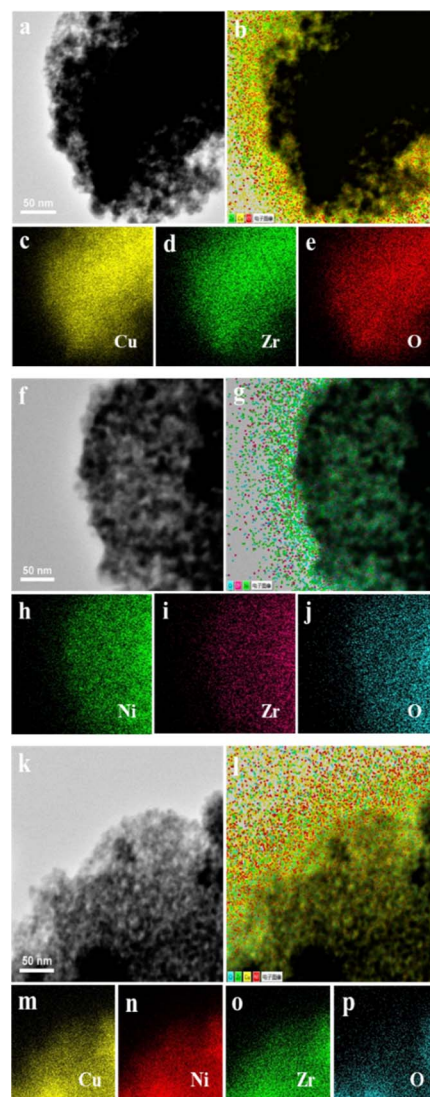vely (Fig. S2†). The peaks located at 932.4 eV and 933.6 are attributed to Cu^0 and Cu^{2+}, respectively.[29] This indicates the Cu on the surfaces of the Cu$_{0.5}$–ZrO$_2$ and Cu$_{0.05}$Ni$_{0.45}$–ZrO$_2$ catalysts was partially oxidized. The Ni 2p spectra of the Ni$_{0.5}$–ZrO$_2$ and Cu$_{0.05}$Ni$_{0.45}$–ZrO$_2$ can be deconvoluted into two peaks, respectively (Fig. S3†). The Ni 2p$_{3/2}$ peak at 852 eV belongs to Ni^0, while the Ni 2p$_{3/2}$ peak at 855 eV is assigned to Ni^{2+}.[30,31] This indicates the Ni on the surfaces of the Ni$_{0.5}$–ZrO$_2$ and Cu$_{0.05}$Ni$_{0.45}$–ZrO$_2$ catalysts was partially oxidized. The Ni^{2+}/Ni^0 ratio for the Ni$_{0.5}$–ZrO$_2$ catalyst calculated from their corresponding peak area is 5.11, while the Ni^{2+}/Ni^0 ratio for the Cu$_{0.05}$Ni$_{0.45}$–ZrO$_2$ catalyst is 4.23, indicating that adding a small amount of Cu into the Ni$_{0.5}$–ZrO$_2$ catalyst can inhibit nickel oxidation.

Catalytic performance

The catalytic performances of the Cu$_{0.5}$–ZrO$_2$, Ni$_{0.5}$–ZrO$_2$ and CuNi–ZrO$_2$ catalysts for LA hydrogenation are summarized in Table 1. The conversions of LA over Cu$_{0.5}$–ZrO$_2$, Ni$_{0.5}$–ZrO$_2$ and CuNi–ZrO$_2$ catalysts were 12.7%, 33.4% and 48.6% at 200 °C

Table 1 Catalytic performance of the $Cu_{0.5}$–ZrO_2, $Ni_{0.5}$–ZrO_2 and CuNi–ZrO_2 for LA hydrogenation[a]

| Entry | Catalyst | LA conv./% | Sel./% | | |
			GVL	HVA[b]	PDO[c]
1	$Cu_{0.5}$–ZrO_2	12.7	>99.9	0	0
2	$Ni_{0.5}$–ZrO_2	33.4	>99.9	0	0
3	$Cu_{0.05}Ni_{0.45}$–ZrO_2	48.6	>99.9	0	0
4	$Cu_{0.125}Ni_{0.375}$–ZrO_2	41.2	>99.9	0	0

[a] Reaction conditions: 15 mg catalyst, 10 mL 5 vol% levulinic acid aqueous solution, 200 °C, 3.0 MPa H_2, 90 min. [b] HVA: 4-hydroxyvaleric acid. [c] PDO: 1,4-pentanediol.

and 3.0 MPa H_2 for 1.5 h, respectively. No reactivity of LA was found in the absence of catalyst. The conversion of LA (33.4%) on $Ni_{0.5}$–ZrO_2 catalyst is almost 3 times as high as that on $Cu_{0.5}$–ZrO_2 catalyst (12.7%) under the same operating conditions, suggesting Ni with higher intrinsic reactivity for LA hydrogenation than Cu. Interestingly, when a small amount of Ni (0.05 mol) in the $Ni_{0.5}$–ZrO_2 catalyst was replaced by Cu, a much higher conversion (48.6%) was achieved under the same reaction conditions. XRD, H_2-TPR and STEM-EDS results show that the replacement of Cu makes NiO in the CuONiO–ZrO_2 easier to reduce and Ni more dispersed in the nanocomposite. We think that the excellent reactivity of the $Cu_{0.05}Ni_{0.45}$–ZrO_2 may be due to a better reducibility of NiO in the CuONiO–ZrO_2 and dispersion of Ni in the $Cu_{0.05}Ni_{0.45}$–ZrO_2 compared to NiO in the NiO–ZrO_2 and Ni in the $Ni_{0.5}$–ZrO_2. Further increasing Cu replacement amount in the $Ni_{0.5}$–ZrO_2 from 0.05 to 0.125 mol had a negligible effect on LA conversion (Table 1). Therefore, the optimum Ni replacement amount with Cu in the $Ni_{0.5}$–ZrO_2 was 0.05 molar fraction.

LA hydrogenation to GVL proceeds *via* consecutive reactions of the formation of 4-hydroxypentanoic acid or angelica-lactones as intermediates.[27] The reaction pathway mostly depends on used catalyst and reaction conditions.[32,33] Various byproducts such as 1,4-pentanediol (PDO) and 4-hydroxyvaleric acid (HVA) are generated from overhydrogenation of GVL when catalyst selectivity is insufficient.[34] Therefore, we pay special attention to identify byproducts in the hydrogenation process of
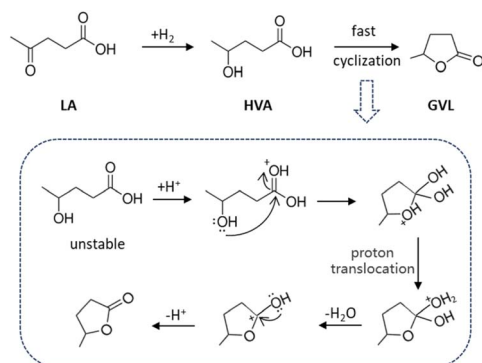
LA using GC-MS. Any byproduct in the reaction mixture is unambiguously detected in our product analysis method. Interestingly, an excellent GVL selectivity (>99.9%) at 100% conversion of LA was obtained on the $Cu_{0.05}Ni_{0.45}$–ZrO_2 at 200 °C and 3.0 MPa hydrogen pressure. Overhydrogenation of the target product GVL, which was observed over other catalysts,[35–37] was thoroughly avoided over the $Cu_{0.05}Ni_{0.45}$–ZrO_2 catalyst (Table 1). It's also worth mentioning that the selectivity of GVL remained at >99.9% throughout the study, which may suggest that the hydrogenation of LA proceeds *via* the formation of unstable HVA, then undergoes rapid cyclization to GVL (Fig. 4). The $Cu_{0.05}Ni_{0.45}$–ZrO_2 also exhibited catalytic activity superior to that of conventional catalysts (Table S2†), showing great potential in sustainable GVL production from LA.

Effect of reaction conditions

We investigated the effects of reaction temperature, H_2 pressure and solvent to ensure the performance of the $Cu_{0.05}Ni_{0.45}$–ZrO_2 catalyst. Fig. 5 shows the performance of LA hydrogenation at different reaction temperatures over the $Cu_{0.05}Ni_{0.45}$–ZrO_2 catalyst. Reaction temperature significantly facilitated LA conversion (Fig. 5). When the reaction temperature rises from 180 °C to 210 °C at 3.0 MPa H_2, the conversion of LA increased nearly threefold (from 18.8% to 57.0%). The selectivity of GVL remained at >99.9% throughout the temperature study. No by-products were detected, which demonstrates that the unde-sired overhydrogenation of GVL to HVA and PDO can be completely suppressed over the $Cu_{0.05}Ni_{0.45}$–ZrO_2 catalyst in a broad window (180–210 °C).

The catalytic performance of $Cu_{0.05}Ni_{0.45}$–ZrO_2 catalyst under different H_2 pressures was evaluated. As displayed in Fig. 6, hydrogen pressure has a remarkable effect on the hydrogena-tion of LA catalyzed by $Cu_{0.05}Ni_{0.45}$–ZrO_2. The LA conversion and GVL selectivity were 13.8% and >99.9% at 1.0 MPa H_2, respectively. When the H_2 pressure increased from 1.0 MPa up to 3.0 MPa, the conversion of LA significantly increased from 13.8% to 48.6%, and the unique selectivity to GVL remained at >99.9%, which suggests that high H_2 pressure favor the hydro-genation of LA to GVL on the $Cu_{0.05}Ni_{0.45}$–ZrO_2 catalyst.

The performance of $Cu_{0.05}Ni_{0.45}$–ZrO_2 catalyst for LA hydro-genation in polar and non-polar solvents was investigated at

Fig. 4 Reaction pathway for LA hydrogenation to GVL over $Cu_{0.05}Ni_{0.45}$–ZrO_2 catalyst.
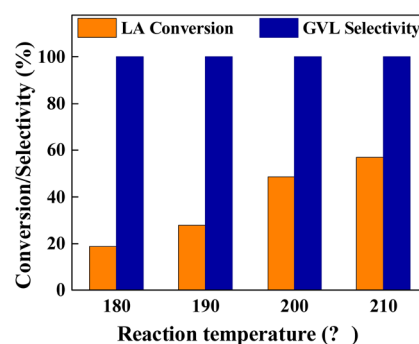

Fig. 5 Catalytic results of the $Cu_{0.05}Ni_{0.45}$–ZrO_2 for LA hydrogenation at various reaction temperatures.
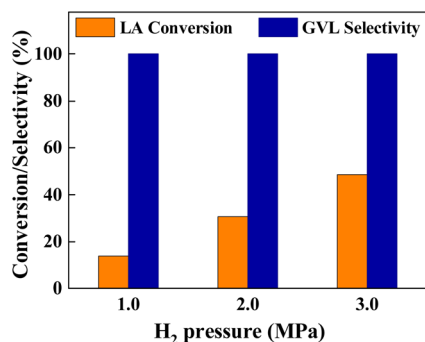
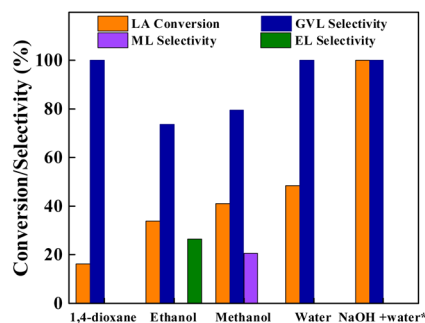Fig. 6 Catalytic results of the Cu$_{0.05}$Ni$_{0.45}$–ZrO$_2$ for LA hydrogenation at various H$_2$ pressures.

Table 2 Effect of NaOH on catalytic performance of the Cu$_{0.05}$Ni$_{0.45}$–ZrO$_2$ for LA hydrogenation[a]

			Sel.%		
Entry	$n_{(NaOH)}/n_{(LA)}$	Conv./%	GVL	HVA[b]	PDO[c]
1	0	18.8	>99.9	0	0
2	1 : 10	30.1	>99.9	0	0
3	1 : 5	46.4	>99.9	0	0
4	1 : 2	32.9	>99.9	0	0

[a] Reaction conditions: 15 mg catalyst, 10 mL 5 vol% levulinic acid aqueous solution, 180 °C, 3.0 MPa H$_2$, 90 min. [b] HVA: 4-hydroxyvaleric acid. [c] PDO: 1,4-pentanediol.
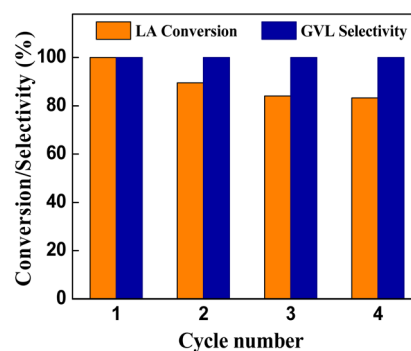

Fig. 7 Catalytic results of the Cu$_{0.05}$Ni$_{0.45}$–ZrO$_2$ for LA hydrogenation in various solvents.

Fig. 8 Reusability of the Cu$_{0.05}$Ni$_{0.45}$–ZrO$_2$ for LA hydrogenation.

200 °C and 3.0 MPa H$_2$, and the data are listed in Fig. 7. Non-polar solvent like 1,4-dioxane showed GVL selectivity of >99.9%, but it exhibited low LA conversion of 16.3%. All polar solvents showed good LA conversion with ethanol, methanol and water as solvents. The substrate reactivity is very different in various solvents with the order of water > methanol > ethanol. The water gave excellent GVL selectivity of >99.9%, whereas methanol and ethanol showed below 80% GVL selectivity, which is owing to the formation of methyl levulinate (ML) and ethyl levulinate (EL) byproducts from the esterification of LA with corresponding solvent alcohol. The different reactivities of LA and GVL selectivity in these solvents on Cu$_{0.05}$Ni$_{0.45}$–ZrO$_2$ catalyst suggest that the solvent polarity have impact on the catalytic performance of the Cu$_{0.05}$Ni$_{0.45}$–ZrO$_2$ catalyst. Polar solvent is more beneficial to LA hydrogenation to GVL on Cu$_{0.05}$Ni$_{0.45}$–ZrO$_2$ catalyst. In particular, when a certain amount of NaOH (n_{NaOH}/n_{LA} = 1 : 5) was added into the same water, however, a very high LA conversion (100%) was achieved under the same reaction conditions, and an excellent GVL selectivity of >99.9% was obtained.

In order to gain further insight into the promotion of NaOH, the effect of different molar ratios of n_{NaOH}/n_{LA} on catalytic performance of Cu$_{0.05}$Ni$_{0.45}$–ZrO$_2$ for LA hydrogenation was investigated at 180 °C and 3.0 MPa H$_2$ (Table 2). The conversion of LA increased from 18.8% to 46.4% when the molar ratio of n_{NaOH}/n_{LA} rose from zero to 1 : 5. Further increasing molar ratios of n_{NaOH}/n_{LA} from 1 : 5 to 1 : 2 had a negligible effect on

the conversion of LA. Therefore, the optimum molar ratio of n_{NaOH}/n_{LA} was 1 : 5. We also studied sodium levulinate hydrogenation to GVL on Cu$_{0.05}$Ni$_{0.45}$–ZrO$_2$ catalyst. The conversion of sodium levulinate is only 1.7% under the same conditions (Table 2), which suggests that an appropriate amount of OH$^-$ can improve activity of the Cu$_{0.05}$Ni$_{0.45}$–ZrO$_2$ catalyst for LA hydrogenation to GVL.

Catalyst reusability

We investigated the reusability of the Cu$_{0.05}$Ni$_{0.45}$–ZrO$_2$ catalyst for the LA hydrogenation to GVL at 200 °C, 3.0 MPa H$_2$ pressure, NaOH solution as a solvent for 1.5 h. After the first LA hydrogenation, the used catalyst was separated, washed using ethanol, dried in vacuum and then used for the next cycle. The results of repeated use three times were shown in Fig. 8. The conversions of LA over fresh, used for second, third, fourth times catalysts were 100%, 89.6%, 84.1% and 83.3%, respectively. After the fourth cycle, the conversion of LA showed a slight downward trend, and the outstanding selectivity of GVL remained at >99.9%. This shows good stability of the catalyst even after 4 cycles.

Conclusions

In summary, we have successfully prepared a highly efficient and reusable Cu$_{0.05}$Ni$_{0.45}$–ZrO$_2$ catalyst for LA hydrogenation to GVL by a simple coprecipitation technique. The LA hydrogenation with Cu$_{0.05}$Ni$_{0.45}$–ZrO$_2$ at 200 °C, 3 MPa for 1.5 h resulted

in 100% LA conversion and >99.9% GVL selectivity, which shows prospects of commercialization. The Ni has higher intrinsic reactivity for LA hydrogenation than Cu, and partly substituting Ni with Cu makes NiO in the CuONiO–ZrO$_2$ easier to reduce and Ni more dispersed in the nanocomposite, which may be responsible for excellent reactivity of the Cu$_{0.05}$Ni$_{0.45}$–ZrO$_2$. An appropriate amount of OH$^-$ can greatly enhance activity of the Cu$_{0.05}$Ni$_{0.45}$–ZrO$_2$ catalyst for LA hydrogenation to GVL.

Data availability

The data supporting this article have been included in the main article and the ESI†.

Author contributions

Yufang Ding: methodology, investigation, writing – original draft. Junli Sun: methodology, investigation, writing – original draft. Rongqi Hu: investigation. Daiping He: supervision, writing – review and editing. Xulin Qiu: investigation, data curation. Chengying Luo: investigation. Ping Jiang: writing – review and editing.

Conflicts of interest

There is no conflict of interest to declare.

Acknowledgements

References

1 P. H. Yan, J. Mensah, M. Drewery, E. Kennedy, T. Maschmeyer and M. Stockenhuber, *Appl. Catal., B*, 2021, **281**, 119470.

2 T. Güney abd and K. Kantar, *Int. J. Sustain. Dev. World Ecol.*, 2020, **27**, 762.

3 I. V. Andreeva, D. H. Zaitsau, S. Qian, V. V. Turovtzev, A. A. Pimerzin, J. E. Bara and S. P. Verevkin, *Chem. Eng. Sci.*, 2022, **247**, 117032.

4 Z. H. Yang, X. Y. Chou, H. Y. Kan, Z. H. Xiao and Y. Ding, *ACS Sustainable Chem. Eng.*, 2022, **10**, 7418.

5 Z. G. Xiao, X. Wang, Z. P. Zhao, Z. Wang, L. L. Gao, Y. Liu and W. G. Zhou, *Catal. Commun.*, 2023, **184**, 106790.

6 D. P. He, Q. Q. He, P. Jiang, G. B. Zhou, R. Q. Hu and W. S. Fu, *Catal. Commun.*, 2019, **125**, 82.

7 H. Liu, X. J. Cao, X. Tang, X. H. Zeng, Y. Sun, X. X. Ke and L. Li, *Green Chem.*, 2021, **23**, 1983.

8 Y. Zhu, Y. Li, S. P. Zhao, R. Jing, H. Q. Zhang, D. L. Sun and S. Sato, *Chem. Lett.*, 2022, **11**, 292.

9 V. S. Jaya, M. Sudhakar, S. N. Kumar and A. Venugopal, *RSC Adv.*, 2015, **5**, 9044.

10 N. Siddiqui, C. Pendem, R. Goyal, T. S. Khan, C. Samanta, K. Chiang, K. L. Shah, M. A. Haider and R. Bal, *Fuel*, 2022, **323**, 124272.

11 A. Patel, J. Pat and S. Pathan, *Inorg. Chem.*, 2023, **62**, 6970.

12 J. R. Wang, Y. Y. Wang, X. L. Tong, Y. W. Wang, G. Q. Jin and X. Y. Guo, *Catal. Commun.*, 2020, **139**, 105971.

13 C. E. Bounoukta, C. Megias-sayago, N. Rendón, F. Ammari, A. Penkova, S. Ivanova, M. A. Centeno and J. A. Odriozola, *Sustain. Energy Fuels*, 2023, **7**, 857.

14 S. Gyergyek, M. Grilc, B. Likozarr and D. Makovec, *Green Chem.*, 2022, **24**, 2788.

15 K. L. Zhang, Q. L. Meng, H. H. Wu, T. Y. Yuan, S. T. Han, J. X. Zhai, B. X. Zheng, C. Y. Xu, W. Wu, M. Y. He and B. X. Han, *Green Chem.*, 2021, **23**, 1621.

16 Z. Ruiz-bernal, M. A. Lillo-ródenas and M. D. Román-martínez, *Catalysts*, 2021, **11**, 559.

17 A. S. Piskun, J. Ftouni, Z. Tang, B. M. Weckhuysen, P. C. A. Bruijnincx and H. J. Heeres, *Appl. Catal., A*, 2018, **549**, 197.

18 J. Feng, X. Gu, Y. Xue, Y. W. Han and X. B. Lu, *Sci. Total Environ.*, 2018, **633**, 426.

19 Z. Y. Li, H. G. Hao, J. J. Lu, C. M. Wu, R. Gao, J. F. Li, C. L. Liu and W. S. Dong, *J. Energy Chem.*, 2021, **61**, 446.

20 K. Sakakibara, K. Endo and T. Osawa, *Catal. Commun.*, 2019, **125**, 52.

21 S. Shao, Z. Z. Ding, C. L. Shang, S. Y. Zhang, Y. C. Ke, G. L. Zhu and Y. Yang, *Chem. Eng. J.*, 2022, **450**, 138153.

22 A. M. Hengne and C. V. Rode, *Green Chem.*, 2012, **14**, 1064.

23 V. Mohan, V. Venkateshwarlu, C. V. Pramod, B. D. Raju and K. S. Rao, *Catal. Sci. Technol.*, 2014, **4**, 1253.

24 H. Q. Wang, H. Chen, B. Ni, K. Wang, T. He, Y. L. Wu and X. Wang, *ACS Appl. Mater. Interfaces*, 2017, **9**, 26897.

25 B. Seemala, C. M. Cai, C. E. Wyman and P. Christopher, *ACS Catal.*, 2017, **7**, 1.

26 S. F. Li, M. X. Li and Y. H. Ni, *Appl. Catal., B*, 2020, **268**, 118392.

27 W. L. Zhang, Y. Yao, S. Q. Xie, K. Gubsch, Y. H. Yang, X. Y. Lan and H. F. Lin, *Catal. Today*, 2021, **374**, 53.

28 H. S. Roh, K. Y. Koo, J. H. Jeong, Y. T. Seo, D. J. Seo, W. L. Yoon and S. B. Park, *Catal. Lett.*, 2007, **117**, 85.

29 P. P. Upare, M. G. Jeong, Y. K. Hwang, D. H. Kim, Y. D. Kim, D. W. Hwang, U. H. Lee and J. S. Chang, *Appl. Catal., A*, 2015, **491**, 127.

30 D. R. Jonesa, S. Iqbala, L. Thomasa, S. Ishikawa, C. Reece, P. J. Miedziak, D. J. Morgan, J. K. Bartley, D. J. Willock, W. Ueda and G. J. Hutchings, *Catal. Struct. React.*, 2018, **4**, 12.

31 P. P. Upare, M.-G. Jeong, Y. K. Hwang, D. Han Kim, Y. D. Kim, D. W. Hwang, U.-H. Lee and J.-S. Chang, *Appl. Catal., A*, 2015, **491**, 127.

32 A. B. Jain and P. D. Vaidya, *Can. J. Chem. Eng.*, 2016, **94**, 2364.

33 O. A. Abdelrahman, A. Heyden and J. Q. Bond, *ACS Catal.*, 2014, **4**, 1171.

34 Y. J. Tsou, T. D. To, Y. C. Chiang, J. F. Lee, R. Kumar, P. W. Chung and Y. C. Lin, *ACS Appl. Mater. Interfaces*, 2020, **12**, 54851.

35 M. Maumela, S. Marx and R. Meijboom, *Catalysts*, 2021, **11**, 292.

36 A. L. Maximov, A. V. Zolotukhina, A. A. Mamedli, L. A. Kulikov and E. A. Karakhanov, *ChemCatChem*, 2018, **10**, 222.

37 L. Xin, Z. Y. Zhang, J. Qi, Z. Y. Zhang, D. Chadderdon and W. Z. Li, *ChemSusChem*, 2013, **6**, 674.